HHS Public Access

Author manuscript

Mater Des. Author manuscript; available in PMC 2019 August 12.

Published in final edited form as:

Mater Des. 2018 August 5; 151: 102–112. doi:10.1016/j.matdes.2018.04.049.

Calcium phosphate coated 3D printed porous titanium with nanoscale surface modification for orthopedic and dental applications

Susmita Bose[*], **Dishary Banerjee**, **Anish Shivaram**, **Solaiman Tarafder**, **Amit Bandyopadhyay**

W. M. Keck Biomedical Materials Research Laboratory, School of Mechanical and Materials Engineering, Washington State University, Pullman, Washington, 99164-2920, USA.

Abstract

This study aims to improve the interfacial bonding between the osseous host tissue and the implant surface through the application of doped calcium phosphate (CaP) coating on 3D printed porous titanium. Porous titanium (Ti) cylinders with 25% volume porosity were fabricated using Laser Engineered Net Shaping (LENS™), a commercial 3D Printing technique. The surface of these 3D printed cylinders was modified by growing TiO_2 nanotubes first, followed by a coating of with Sr^{2+} and Si^{4+} doped bioactive CaP ceramic in simulated body fluid (SBF). Doped CaP coated implants were hypothesized to show enhanced early stage bone tissue integration. Biological properties of these implants were investigated *in vivo* using a rat distal femur model after 4 and 10 weeks. CaP coated porous Ti implants have enhanced tissue ingrowth as was evident from the CT scan analysis, push out test results, and the histological analysis compared to porous implants with or without surface modification via titania nanotubes. Increased osteoid-like new bone formation and accelerated mineralization was revealed inside the CaP coated porous implants. It is envisioned that such an approach of adding a bioactive doped CaP layer on porous Ti surface can reduce healing time by enhancing early stage osseointegration *in vivo*.

Keywords

3D printing; porous cylinders; surface modification; titania nanotubes; *in vivo* osseointegration; accelerated healing

[*] sbose@wsu.edu.

7.0 Data Availability

The raw data required to reproduce these findings are incorporated in this manuscript.

Supplementary figure shows XRD peaks of the doped and undoped CaP coating.

1.0 Introduction

Titanium (Ti) is a widely used metallic biomaterial that is bio-inert [1]. Excellent fatigue and corrosion resistance[2] along with high strength-to-weight ratio makes Ti an ideal metal for load-bearing implants [1]. In spite of commendable progress in the field of metallic orthopedic biomaterials, host bone and implant integration still need improvement to minimize healing time and increase implant lifetime *in vivo*. Among others, mismatch of Young's moduli, also known as stress shielding, between the bulk metallic materials like Ti (110 GPa), Co-Cr alloys (230 GPa) and bone (10–30 GPA) has been recognized as one of the reasons for implant loosening [3]. To enhance *in vivo* lifetime of implants, it is envisioned that modifying surface properties can improve tissue materials interactions and subsequent healing. Weber et al. reported usage of porous materials to enhance osseointegration in 1972 [4] and henceforth substantial research has been done in the development of porous materials [3,5,6,7] for biomedical usages. To augment further cell adhesion and tissue ingrowth, research has also been devoted to nanoscale surface modification of the implants [8, 9]. One of the common methods to perform nanoscale surface modification is by the growth of nanotubes on the surface of the metallic implants because of the process simplicity and flexibility in terms of controlling the parameters [10, 11, 12]. Previous works have shown that excellent biocompatibility with higher surface to volume ratio and surface chemistry of the nanotubes has enhanced cell growth and proliferation and prevented bacterial infection [10–14]. TiO_2 nanotube (TNT) film formation on porous titanium also makes the surface more hydrophilic and plays a role in improving surface chemistry and hence cell adhesion [15]. While the TNT lowers the contact angle of Ti surface from ~ 70 degrees in Ti to below 20 degrees in DI media, and subsequently increases the surface energy, it doesn't add bioactivity as seen in the case of CaP coated Ti implants [11].

CaP coatings on metallic implants help overcome associated limitations such as lack of tissue integration [16–19]. Figure 1 shows the gradual effects of the combination of doped CaP coating with nanoscale surface modification of porous Ti on early stage osseointegration in a rat distal femur model. The nanoscale surface modification along with the CaP coatings will be performed on the stem regions of a total hip or knee arthroplasty to initiate early bone integration at the implant interface, eventually leading to accelerated healing [20].

Ceramic coatings have been done in numerous methods like plasma spray coating, biomimetic coatings and sol gel coatings [18, 21, 22]. Each of these coating techniques comes with their own pros and cons [23]. Biomimetic coating involves the immersion of the metallic implants in simulated body fluid at physiological pH and temperature [23]. It also comes with an inherent advantage of not been a line of sight technique and hence is able to successfully and homogeneously coat porous metallic scaffolds [23]. CaP apatite has also been shown to form on metallic implants, glasses in metastable SBFs [24]. Na^+, Mg^{2+}, Sr^{2+}, Zn^{2+} and Si^{4+} like metallic ions have been found in the mineral phases of natural bone [25–26]. Several works done by many groups, including ours have also aimed to enhance the *in vitro* and *in vivo* osseointegration, mechanical properties, wear degradation properties by the incorporation of inorganic cations in CaP coatings [16, 18, 25, 27]. The enhancement of

bone regeneration is reported with the incorporation of strontium ions in synthesized bone implants [16, 28, 29]. Sr^{2+} inhibits bone resorption due to osteoclast activity and intensifies the bone regeneration by augmenting osteoblast activity eventually leading to bone formation [30–31]. Strontium ion has also been used as an osteoporotic drug due to its simultaneous stimulatory effect on bone remodeling [32]. Strontium induces osteogenesis by increased formation of β-catenin [26]. Silicon ion, found frequently in connective tissue and bone of the body, structurally stabilizes collagen and influences early stage bone formation [27, 33]. Reports have described the influence of silicon on bone formation by the dependence of bone mineral density on intake of silicon [34]. However, a knowledge gap still exists for combined effects of TiO_2 with CaP, with or without dopants on early stage osteogenesis.

Additive manufacturing or 3D printing (3DP) comes with a variety of solutions to manufacturing limitations of conventional techniques. 3DP can be on-demand, site specific and allow better porosity control [35,36, 37]. Laser based solid freeform technique Laser Engineered Net Shaping (LENS™) has been utilized to develop the porous Ti cylinders used in this study. Since LENS is not a powder bed process, and the powder delivery happens through forced Ar gas, only metallurgically bonded particles bond together and loose powders are blown away. Nanotube films were grown by electrochemical anodization and metallic ion doped calcium coating was done by biomimetic coating technique. Nanoscale modification of the Ti implants does not interact with the physiological system, however, the mismatch of mechanical properties between the ceramic based coating and the metallic implant is minimized [38]. This plays an important role in improving the adhesion of the calcium phosphate coating on the metallic implants and prevents delamination of the coating *in vivo*. The objective of this study was to understand the influence of doped CaP coating on 3DP porous Ti implants with or without TiO_2 layer towards the early stage osteogenesis. Addition of TNT on LENS processed porous implants with doped CaP is novel and the doped CaP coating on surface modified porous Ti implants was hypothesized to enhance osseous tissue ingrowth at the interface of the implants *in vivo*. Male Sprague-Dawley rats were implanted for 4 and 10 weeks. Samples were characterized via mechanical push out tests, histological imaging, histomorphometric analysis, computed topography, and scanning electron microscope imaging to measure the influence of surface modification on early stage osseointegration.

2.0 Materials and Methods

2.1 Fabrication of porous samples using LENS™

Porous Ti rods of 3.00mm average diameter were fabricated for *in vivo* analysis using CAD software, referred as LENS porous Ti henceforth. The software was utilized to design cylinders of 75mm in length and average diameter of 2.3 mm. The diameter of the cylinders in the developed CAD design was too small to incorporate any kind of designed porosity, therefore, the powder was partially melted using low power of the laser to create the porosity in the cylinders. The developed CAD design was uploaded to the LENS™ motion control software and further translated into tool path files for processing. Figure 2 shows a schematic design of the LENS™ [10]. Commercially pure titanium powder (ATI Powder

Metals, Pittsburg, PA, USA), 99.99% pure, having spherical particles of average diameter of 44μm to 149μm was used for the fabrication of the cylinders. Similar 99.99% commercially pure 3mm thick titanium plate (President Titanium, Hanson, MA USA) was used as the substrate for the building of the cylinders. Fabrication of the cylinders had been achieved using the LENS™ system (Optomec Inc., Albuquerque, NM USA) armed with continuous wave Nd:YAG laser capable of generating a maximum power of 500W. Laser was focused on the substrate to melt and create a melt-pool where metal powders were added to increase the volume of the melt pool. The substrate was moved in X and Y direction to write with the molten metal. After each layer, laser moved up in the Z-direction and continue the build on top of the previous layer. After each batch was processed, the porosity was measured using Archimedes' method. The processing parameters for fabrication were further altered based on the measured porosity of the cylinders. Several such endeavors led to a success in producing the porous Ti rods with a laser power of 280W and raster scanning speed of 60cm/min to 80cm/min. During the fabrication process, the oxygen level was measured by a sensitive oxygen analyzer and was maintained below 10ppm to avoid any chances of oxidation during processing. To provide surface finish, samples were slightly ground on wet 500 grit SiC paper. Several cylinders of average length of 5.00–5.50 mm were cut out from the fabricated cylinders and rinsed with series of deionized water after ultrasonic cleaning in 100% ethanol for 20 mins and blow dried with warm water.

2.2 Nanotubes formation

Electrochemical anodization was used to develop TiO_2 nanotube film on the LENS™ fabricated porous titanium cylinders at room temperature, referred as LENS™ porous Ti-NT. The cathode consisted of $1mm^2$ platinum foil, the anode was the porous Ti cylinders and the electrolyte was 1% HF in deionized water solution. Throughout the process of growing nanotubes, voltage was continuously maintained at 20V for 60 mins by DC power supply from Hewlett Packard (0–60 V/0–50 A, 1000 W). The cylinders were rinsed thoroughly with deionized (DI) water before further treatment.

2.3 Calcium phosphate coating

Biomimetic coating method was utilized to coat the surface modified porous scaffolds because of its inherent advantage of not a line of sight technique. Porous LENS™ processed Ti-NT cylindrical rods were kept immersed into 10 mL of 10x simulated body fluid (SBF) for 72 h in static condition at 37 °C. SBF were changed every 24 h. Specimens were taken out from SBF after 72 h followed by three times gentle washing in 2 mL DI water. Specimens were then air dried and coating morphologies were observed under SEM. These samples are hence referred as LENS™ porous Ti-NT-CaP. To prepare Sr^{2+} and Si^{4+} doped CaP coating, 2.1 atomic wt.% Sr^{2+} (equivalent to 1 wt.% SrO and 0.5 wt% SiO_2 doped in HA) and 0.006 wt.% Si^{4+} (equivalent to 1 wt.% SrO and 0.5 wt% SiO_2 doped in HA) were added in the form of $SrCl_2.6H_2O$ and Na_2SiO_3 in 10x SBF [39]. After that, a similar procedure was followed as described above for CaP coating and the fabricated cylinders are alluded as LENS™ porous Ti-NT-CaP-Sr-Si.

2.4 *In vivo* study

2.4.1 Surgery and implantation procedure—All surgical and experimental procedures have been performed in accordance to protocols approved by the Institutional Animal Care and Use Committee (IACUC) of Washington State University. Male Sprague Dawley rats (Simonsen Laboratories, Gilroy, CA, USA) each weighing around 280–300 gms underwent bilateral surgery for the entire set of the study. The rats were kept in properly labelled individual cages and acclimatized in humidity and temperature controlled rooms with alternate 12-hour cycles of light and darkness. The rats were anesthetized with IsoFlo® (Isoflurane, USP, Abbott Laboratories, North Chicago, IL, USA) coupled with an oxygen (Oxygen USP, A-L Compressed Gases Inc., Spokane, WA, USA) regulator. Proper surgical anaesthesia conditions were ensured by monitoring through pedal reflex and respiration rate. Drill bits of diameter similar to that of the cylindrical implant were used to generate a defect in the distal femur of the rat and the defect was thoroughly rinsed with saline water to clear any remaining bone particles. The cylinders were implanted by press fit and the incision was sutured by undyed braided coated VICYRL-polyglactin 910 synthetic surgical suture. (Ethicon Inc., Somerville, NJ, USA) Meloxicam injection was administered following the surgery to reduce pain and chances of any infection were prevented by application of disinfectant around the incision region. On completion of 4 weeks and 10 weeks after surgery, an over dosage of isoflurane was used for euthanization.

2.4.2 CT scan analysis and interfacial strength by push out test—Radiographic images were acquired from X-ray energy source on the IVIS® Spectrum CT and further scanned by 40 μm voxel size and 150 resolution to create a three-dimensional volume. The obtained 3D scans are further fed into Living Image® Software 4.4 to generate the three-dimensional images. 2 samples of each composition after 10 weeks of implantation were used for the CT Scan.

Push out tests were done with the aim of calculating the shear modulus between the growing tissue along the implant surface and the implant itself. An idea of the shear modulus will help determine the bonding strength between the host tissue and implant surface. Shear modulus were calculated from the slope of the shear stress vs. shear strain plots. Push out tests were performed using a 136.07 kg load cell with a servo-hydraulic controlled Instron 3343 load frame at a 0.33 mm/sec cross-head speed. This test frame is capable of 1 kN tensile, compression, 3-point bending, or peel tests. 2 implants at each composition and time point were used for the push out test. Figure 3 shows the schematic and image of our test fixture designed and built at WSU. To maintain proper alignment during testing, we have a clamping arrangement for the samples that can avoid any translational motion along X and Y direction when the load is applied from the Z-direction. Interfacial shear modulus values were calculated from the linear region of the stress vs. strain plot generated from the load-displacement data. Harvested bone samples were wrapped in a gauze pre-wet with saline and brought to the test location immediately for push-out test.

2.4.3 Histology, histomorphometry and SEM characterization—Post-surgery, the clipped bone-implant composites were fixed immediately in 10% formalin solution to allow tissue preservation. After 72 hours of immersion, they were dehydrated in a

consecutive series of ethanol drying using 70%, 95%, and 100%, 1:1 acetone-ethanol solution, and finally 100% acetone. The samples were then embedded into Spurs resin and thin slices were cut out using a diamond blade. The sections were rinsed with water and mounted on glass slides before being stained with a modified Masson Goldner's trichrome staining method [24]. The stained tissue implant interface was observed under light microscope (Olympus BH-2, Olympus America Inc., USA). At least 5 sections from different rats were used for the histology images and follow-up histomorphometric analysis. Histophormetric analysis had been performed as a quantitative analysis of the histology images from ImageJ to study the total osteoid formation and the total bone formation at the interface of the implant using 3 images [200μm by 200μm] from each section, i.e., 15 images for each datum presented here. A region of 80 μm in radius has been selected around the implant to study the bone interlocking and effects of the compositions on the osteoid formation in the region surrounding the bone from three different images. The data has been normalized over the diameter of the implant. The percentage of the osteoid formation and total volume of bone formation were plotted against the different compositions at the two-time points. For further clarity, the interface of all the cut sections described above was observed under FESEM (FEI Quanta 200, FEI Inc., OR, USA), at low voltage of 10kV and low vacuum.

3.0 Results

3.1 Surface Morphology of LENS™ processed porous Ti implants, nanotubes and CaP coating

SEM images of LENS™ processed porous Ti rods along with grown nanotubes film before and after calcium phosphate coating have been described in Figure 4. The volume porosity of the fabricated implant was approximately 25%. A macro image of the LENS processed Ti implant has been shown in figure 4 (a) [24]. Pore sizes were measured from the scanning electron microscopy (SEM) image shown in figure 4 (b) and was found to be in the range of 200–300 μm, in accordance to our previous studies [7, 24]. Previously, we have also analyzed the Young's modulus of LENS™ processed porous Ti structures and observed them in the range of 2– 44 GPa, which is similar to that of human cortical bone, 7–30 GPa [7]. Also, the mechanical strength for these porous structures tend to vary from 24 to 463 MPa [7]. Porosity of the processed cylinders have been measured to be 25% by Archimedes' method. After anodization, the length of the nanotubes has been measured to be 375±35 nm and the diameter around 105±30 nm as evident from Figure 4c.

Figure 4 (d) and (e) show the morphology and thickness of the of Sr- and Si doped CaP coating. CaP coating thickness measurement was done on planar Ti substrate under similar conditions for CaP coating on LENS™ Porous Ti-NT. The thickness of the CaP coating has been observed to be around 120 nm and that of the doped CaP coating as 170 nm. Since the CaP and doped CaP coatings are done using biomimetic process, uniformity in the dopant concentration was achieved. Moreover, the CaP coating strongly adhered to the nanotubes.

3.2 Histological evaluation

Biocompatibility, new bone formation, and mineralization were analyzed by histological evaluations to study the effects of the nanotube film and CaP coating on porous Ti cylinders after 4 and 10 weeks, seen in Figure 5. Osteoid-like new bone formation has been observed even at the 4 weeks' time point. The orange-reddish color around the implant at the early time point indicates osteoid formation without any cytotoxicity around the area of implantation. Mineralized bone has been observed by the greenish color and nuclei have been stained with bluish black spots. More osteoid formation has been noticed after 10 weeks of implantation on the CaP coated porous Ti rods. No visible gaps of osteoid formation have been seen around the area of implantation. Sr^{2+} and Si^{4+} doped CaP coated Ti rods have shown more osteoid formation after 10 weeks of implantation compared to Ti rods with nanotube film. Early stage osteogenesis was noticed proving that there was no cytotoxic effect due to the implantation. From Figure 6 (a) and (b), almost 100 % bone formation and higher osteoid formation have been noticed after 10 weeks in undoped and doped CaP coated samples compared to around 60% bone formation in control samples. The effects of compositions in the interfacial bone formation has been more pronounced in the early time points, compared to the later time points. Thus, by the combinations of titania nanotubes with doped CaP coating, we have been able to achieve accelerated bone formation in 4 weeks which can be compared to the bone formation in control samples in 10 weeks. This further indicates towards the strong bone interlocking and confirms presence of no gaps at the implant interface in the CaP coated implants as early as 4 weeks.

3.3 CT scan and push out test analysis

To detect any visible gaps or defects at the interface of the bone tissue and implant, CT scan analysis was executed on few samples, shown in Figure 7. Proper bone lodging into the implant is seen in the cylinders with metallic ion doped CaP coating. Images show the effect of the porosity on the osseointegration but are limited by the machine related resolution issues. However, no signs of defects or cytotoxicity is noted from the CT scan analysis which is an indication of good osteogenesis.

Interfacial shear modulus values were calculated from the push out tests to analyze the interfacial bonding strength between the implant and bone tissue. After 4 weeks of implantation, the shear modulus in CaP coated porous Ti rods with and without dopants was almost 4 times (~80 MPa) compared to porous Ti with or without nanotubes (~26 MPa). Increased shear modulus values after 10 weeks of implantation compared to 4 weeks prove more osseointegration gradually with time. Shear modulus values (~110 MPa for all compositions) after 10 weeks of implantation may not be an appropriate reflection of the actual mechanical interlocking because the bone broke while performing the push out tests in all cases.

3.4 SEM characterization

SEM images of porous Ti with and without nanotube film are shown in Figure 8(A) and 8(B). Some notable gaps are seen at the interface of the bone tissue and implant for both samples 4 weeks after implantation. These gaps have been seen to heal over time and notably less gaps are seen after 10 weeks of implantation. SEM micrographs of CaP coated

porous Ti rods with nanotube film are shown in Figure 8(C). Osteoid formation has been seen even after 4 weeks of implantation shown by the color contrast. Notable gaps were not seen at the interface proving good osseointegration. Figure 8(D) shows Sr^{2+} and Si^{4+} doped CaP coated Ti rods with nanotube film. From the comparison of the SEM images at the interface of the host tissue and the implant, it is noted that visible gaps at the interface considerably decrease from the 4 weeks to 10 weeks' time point. Cylinders with doped metallic ions show strong bonding at the interface with no noticeable gaps after 10 weeks of implantation. This also signifies much improved bonding of the host tissue with the implant with the usage of Sr^{2+} and Si^{4+} doped CaP coated Ti rods compared to porous Ti rods with nanotube films.

4.0 Discussion

Often, metallic implant failures have been attributed to the lack of early stage osteogenesis [40]. Interconnected porosity in scaffolds influences the tissue ingrowth and enhances lifetime of the implant by improving the biological properties. Connected pores are also helpful in transporting metallic wastes and exchanging of nutrients and blood and hence crucial for vascularization [28]. LENS™ has been categorized under directed energy based additive manufacturing technique by ASTM Standards for Terminologies for Additive Manufacturing, F2792–12a [41]. It is a directed energy based deposition technique and had been used to fabricate primarily metallic parts or metallic composite parts from powdered materials. The desired part is designed into a CAD software and fed into the machine to be converted into motion control designs which influences the actual build design [35, 37]. The multi-hopper system incorporated in the LENS™ allows usage of multi-material and control of the process parameters and laser power allow fabrication of various complex geometry. Partial melting of the powder and usage of low laser power also allow fabrication of *in situ* porosity.

The experimental procedures optimized in the present study have been able to fabricate titanium implants with random porosity to mimic the structure of the natural bone. The primary objective of the study was to induce early stage osteogenesis and tissue ingrowth at the interface of the implant and host bone tissue in the presence of a combination of nanotubes and doped CaP coating on porous metallic scaffolds.

Previous reports have demonstrated that an optimal porosity of more than 20% is required for effective osseous tissue integration [42, 43]. This study had been able to optimize the process parameters of the LENS™ system and was able to fabricate porous Ti rods with porosity of around 25% keeping up with the requirement of porous implants [24]. Scaffolds fabricated with 25 – 42% porosity can be modified to possess mechanical properties like compressive strength and Young's modulus similar to cortical bone [44] and improve the implant life *in vivo*. Pores greater than 200 μm allow the migration of osteoprogenitor cells into the scaffolds and lowers the overall scaffold density. This is crucial in reducing the mismatch of stiffness between the metallic implant and surrounding osseous tissue [17, 45].

Rough surfaces facilitate enhanced osteoblast cell attachment and differentiation compared to an untreated surface [17, 44]. Nanoscale surface modification by the growth of titanium

nanotube film has been one of the most commonly used methods to promote early stage osseointegration [8]. The higher surface to volume ratio also helps in making the surface hydrophilic which probes as a perfect environment for osteoblast cell attachment. CaP coating has also been done on the surface modified titanium implants to improve the bioactivity of the implants [45]. In many cases, CaP coated implants suffer from lower adhesive strength and delaminates *in vivo* within a short period of implantation. The presence of the nanoscale modification by the titanium nanotubes is crucial in reducing the mechanical mismatch between the ceramic coating and metallic implants [24]. This improves the coating quality and prevents the coating delamination *in vivo*. This study aims to address the knowledge gap, should the doped CaP coating in the presence of nanotubes enhance the early stage osseointegration.

The increased bone formation by the presence of the dopants has been demonstrated in the histology analysis presented in Figure 5 and 6. Push out tests were performed to validate our histological data in terms of bone tissue adherence and related mechanical strength of implants. Push-out tests are more relevant in rabbit or other large animal models where larger cross-section of bone is available to interact with the implant. However, our aim was to have some preliminary information to see if push-out data can correlate with the histology, and only used n=2. Push out test results after 4 weeks of implantation show a higher shear modulus value for the doped CaP coated samples revealing stronger bonding between the host tissue and implant in the case of the doped CaP samples compared to the pure ones. With the addition of CaP, the shear modulus increased from 25.82 MPa in LENS™ porous Ti to 80.09 MPa within 4 weeks of implantation. The low number of samples (n=2) did not allow us to run a full-scale statistical analysis, however, a variation in shear modulus from 25.82 MPa to 80.09 MPa may not need a statistical analysis to appreciate the significant variation due to surface treatment. Moreover, it is in conjunction with other characterization tools and techniques, and not an outlier. However, as mentioned before, the shear modulus values obtained after 10 weeks of surgery may be looked upon as the strength borne by the bone before cracking (around 110 MPa) and not a direct reflection of interfacial bonding at the tissue interface. As we have seen before [10, 46], surface treated implants are difficult to dislodge after about 8 weeks of implantation in rat distal femur model and a bone fracture is common in those cases. Most typically, bone fracture occurs at or higher than 100 MPa, which is in line with the findings in our previous studies [10, 46]. The interfacial strength between the bone tissue and the implant remained intact until the bone broke in all cases, therefore it can be stated that the interfacial bonding strength is higher than 110 MPa.

This shows that the combination of CaP coating with the nanotubes could enhance early stage osseointegration significantly, similar to those achieved by the porous LENS™ Ti after 10 weeks after implantation. Tremendous enhancement of early stage osteogenesis was observed through tailoring chemistry and dopant chemistry with no usage of any growth factors. No significant effects of the addition of dopants in CaP were noticed from the push out test results and no cytotoxicity was observed. It was believed that the amount of dopants was too small and it was overshadowed by the combined effects of TiO_2 and CaP coating. This highlighted the effects of the addition of CaP on titanium nanotubes in porous metallic implants. However, the push out tests after 10 weeks of implantation may not be an

appropriate contemplation as discussed previously. Reports have shown that bones can withstand a maximum shear modulus of 130–180 GPa [29], after which cracking will occur. In this study, as after exceeding the maximum shear modulus value, the bone broke. The mechanical interlocking at the interface of the bone tissue and implant was strong enough to withstand forces more than what the natural bone could. Enhanced osteogenesis and early bone formation was observed by the presence of the doped CaP and the porous implant, which held the implant strong enough to allow the bone to break under shear conditions without affecting the mechanical interlocking at the interface.

The quantitative push out tests can be more substantiated by the qualitative histology and CT scan results. The interconnected pores and the nanotube film on the porous surface provide a high surface area, which is useful for the stronger mechanical interlocking of the implant into the natural bone tissue and is in line with previous findings [47]. New bone formation was noticed through the induction of osteoid formation by the rough surface created by the pores. Considerable gaps are visible in the uncoated porous cylinders when compared to the ceramic coated scaffolds. Signs of bonding and tissue ingrowth are seen in the CaP coated cylinders from the computer tomography scans. Histomorphometric analysis done using ImageJ software from the histology micrographs also show 100% bone formation in the regions adjacent to the implant, further proving the absence of gaps in the CaP coated samples. CT scan images do not present any visible gaps or defects in the doped CaP coated implants. Proper bone lodging had been noticed in the implant even at the early time point for all the compositions. Tissue in-growth in the porous cylinders was evident from these images. SEM images show similar gaps in the porous Ti compared to the CaP coated Ti. Almost complete bone bonding has been seen in the CaP coated samples 4 weeks after implantation, similar to the porous Ti, 10 weeks after implantation.

Porous metallic implants have been fabricated through laser processed 3D printing. These results show that strontium oxide and silicon oxide doped calcium phosphate coated porous Ti rods with nanotube film enhance the early stage osseointegration and improves mechanical interlocking between the host bone and implant compared to pure porous Ti rods. Hence the study could successfully lead to accelerated healing by enhancing osteogenesis in a bone defect repair model in a rat distal femur.

5.0 Conclusions

Ti rods, with interconnected random porosity of around 25 volume percent with and without nanoscale surface modification, have been 3D printed using LENS™ to analyze the effects of surface modification on the bonding strength at the interface between the implant and the osseous tissue, and early stage osseointegration in vivo. The porous surface modified titanium was further coated with doped calcium phosphate to enhance osseointegration, and then implanted into a rat distal femur model for 4 and 10 weeks. Shear modulus values, computed from the push out tests, revealed high values of 80.09 MPa for LENS porous Ti-NT-CaP compared to the 25.85 MPa for porous Ti after 4 weeks of implantation divulging evidences of enhanced early stage osteogenesis. After 10 weeks of implantation, evidence of fully integrated implants was demonstrated due to bone fracture during push out tests. Histological micrographs, CT scan analysis and SEM images also confirmed that CaP Ti

cylinders showed enhanced osteogenesis and strong interfacial bonding at the interface of the bone tissue. The effects of dopants were overshadowed by the combined effects of titanium nanotubes and CaP coating. Porous Ti implants with TiO_2 nanotubes induced early stage osteogenesis while the addition of calcium phosphate coating further enhanced defect healing and mechanical interlocking at the interface.

Supplementary Material

Refer to Web version on PubMed Central for supplementary material.

Acknowledgements

Authors would also like to acknowledge financial support from the National Institute of Arthritis and Musculoskeletal and Skin Diseases of the National Institutes of Health under grant numbers R01 AR066361 and R01 AR 067306 and does not have any possible conflict of interest. The authors would like to thank Dr. Himanshu Sahasrabudhe for his help with the metallic implant fabrication using the LENS™ and Valerie Lynch-Holm and Dan Mullendore at Franceschi Microscopy & Imaging Center, Washington State University for their help with histology imaging. The content is solely the responsibility of the authors and does not necessarily represent the official views of the National Institute of Health.

8.0 References

1. Bose S, Banerjee D, & Bandyopadhyay A (2017). Introduction to biomaterials and devices for bone disorders. In Materials for Bone Disorders (pp. 1–27).
2. Mercado C, Seeley Z, Bandyopadhyay A, Bose S, & McHale JL (2011). Photoluminescence of dense nanocrystalline titanium dioxide thin films: effect of doping and thickness and relation to gas sensing. ACS applied materials & interfaces, 3(7), 2281–2288. [PubMed: 21702459]
3. Taniguchi N, Fujibayashi S, Takemoto M, Sasaki K, Otsuki B, Nakamura T, … & Matsuda S (2016). Effect of pore size on bone ingrowth into porous titanium implants fabricated by additive manufacturing: an in vivo experiment. Materials Science and Engineering: C, 59, 690–701. [PubMed: 26652423]
4. Weber JN, White EW, Carbon-metal graded composites for permanent osseous attachment of non-porous metals. Materials Research Bulletin, 1972, 7(9), 1005–1016.
5. Clemow AJT, Weinstein AM, Klawitter JJ, Koeneman J, & Anderson J (1981). Interface mechanics of porous titanium implants. Journal of Biomedical Materials Research Part A, 15(1), 73–82.
6. Guyer RD, Abitbol JJ, Ohnmeiss DD, & Yao C (2016). Evaluating osseointegration into a deeply porous titanium scaffold: a biomechanical comparison with PEEK and allograft. Spine, 41(19), E1146–E1150. [PubMed: 27135643]
7. Xue W, Krishna BV, Bandyopadhyay A, Bose S, Processing and biocompatibility evaluation of laser processed porous titanium. Acta biomaterialia, 2007, 3(6), 1007–1018. [PubMed: 17627910]
8. do Amaral Escada AL, Trujillo N, Popat KC, & Rosifini Alves Claro AP (2017). Human Dermal Fibroblast Adhesion on Ti-7.5 Mo after TiO2 Nanotubes Growth In Materials Science Forum (Vol. 899, pp. 195–200). Trans Tech Publications.
9. Maggi A, Li H, & Greer JR (2017). Three-dimensional nano-architected scaffolds with tunable stiffness for efficient bone tissue growth. Acta biomaterialia, 63, 294–305 [PubMed: 28923538]
10. Bandyopadhyay A, and Bose S, “Modified metal materials, surface modifications to improve cell interactions and antimicrobial properties, and methods for modifying metal surface properties.” U.S. Patent No. 8,545,559 1 Oct. 2013.
11. Das K, Bose S, and Bandyopadhyay A, TiO_2 nanotubes on Ti: influence of nanoscale morphology on bone cell–materials interaction. J. Biomed. Mater. Res. Part A 2009, 90(1), 225–237.
12. Liu W, Su P, Chen S, Wang N, Ma Y, Liu Y, … & Webster TJ (2014). Synthesis of TiO 2 nanotubes with ZnO nanoparticles to achieve antibacterial properties and stem cell compatibility. Nanoscale, 6(15), 9050–9062 [PubMed: 24971593]

13. Bandyopadhyay A, Bernard S, Xue W, Bose S, Calcium Phosphate-Based Resorbable Ceramics: Influence of MgO, ZnO, and SiO_2 Dopants. Journal of the American Ceramic Society, 2006, 89(9), 2675–2688
14. Raphel J, Holodniy M, Goodman SB, & Heilshorn SC (2016). Multifunctional coatings to simultaneously promote osseointegration and prevent infection of orthopaedic implants. Biomaterials, 84, 301–314. [PubMed: 26851394]
15. Brammer KS; Oh S; Cobb CJ; Bjursten LM; van der Heyde H; Jin S Improved bone-forming functionality on diameter-controlled TiO 2 nanotube surface. Acta biomaterialia, 2009, 5(8), 3215–3223 [PubMed: 19447210]
16. Fielding GA, Roy M, Bandyopadhyay A, and Bose S, Antibacterial and biological characteristics of silver containing and strontium doped plasma sprayed hydroxyapatite coatings. Acta biomaterialia, 2012, 8(8), 3144–3152. [PubMed: 22487928]
17. Hench LL. Bioceramics: from concept to clinic. J Am Ceram Soc 1991, 74, 1487–1510.
18. Nguyen HQ, Deporter DA, Pilliar RM, Valiquette N, and Yakubovich R "The effect of sol–gel-formed calcium phosphate coatings on bone ingrowth and osteoconductivity of porous-surfaced Ti alloy implants." Biomaterials 25, no. 5 (2004): 865–876.
19. Goodman SB, Yao Z, Keeney M, & Yang F (2013). The future of biologic coatings for orthopaedic implants. Biomaterials, 34(13), 3174–3183 [PubMed: 23391496]
20. Dadsetan M, Guda T, Runge MB, Mijares D, LeGeros RZ, LeGeros JP, … & Yaszemski MJ (2015). Effect of calcium phosphate coating and rhBMP-2 on bone regeneration in rabbit calvaria using poly (propylene fumarate) scaffolds. Acta biomaterialia, 18, 9–20. [PubMed: 25575855]
21. Denry I, & Kuhn LT (2016). Design and characterization of calcium phosphate ceramic scaffolds for bone tissue engineering. Dental Materials, 32(1), 43–53. [PubMed: 26423007]
22. Zyman Z, Weng J, Liu X, Zhang X, and Ma Z "Amorphous phase and morphological structure of hydroxyapatite plasma coatings." Biomaterials 14, no. 3 (1993): 225–228.
23. Barrere F, Layrolle P, Van Blitterswijk CA, De Groot K, Biomimetic coatings on titanium: a crystal growth study of octacalcium phosphate. Journal of Materials Science: Materials in Medicine, 2001, 12(6), 529–534 [PubMed: 15348269]
24. Bandyopadhyay A, Shivaram A, Tarafder S, Sahasrabudhe H, Banerjee D, Bose S, In vivo response of laser processed porous titanium implants for load-bearing implants. Annals of Biomedical Engineering, 2016, 1–12. [PubMed: 26620776]
25. Pabbruwe MB, Standard OC, Sorrell CC, & Howlett CR (2004). Bone formation within alumina tubes: effect of calcium, manganese, and chromium dopants. Biomaterials, 25(20), 4901–4910. [PubMed: 15109850]
26. Norhidayu D, Sopyan I, & Ramesh S (2008). Development of zinc doped hydroxyapatite for bone implant applications. In ICCBT 2008 Conference (pp. 257–270)
27. Fielding G and Bose S, SiO_2 and ZnO dopants in three-dimensionally printed tricalcium phosphate bone tissue engineering scaffolds enhance osteogenesis and angiogenesis in vivo. Acta biomaterialia, 2013, 9(11), 9137–9148. [PubMed: 23871941]
28. Karageorgiou V, Kaplan D, Porosity of 3D biomaterial scaffolds and osteogenesis. Biomaterials 2005, 26(27):5474–5491, 2005.
29. Yang F, Yang D, Tu J, Zheng Q, Cai L, Wang L, Strontium Enhances Osteogenic Differentiation of Mesenchymal Stem Cells and In *Vivo* Bone Formation by Activating Wnt/Catenin Signaling. Stem Cells, 2011, 29, 981–991. doi:10.1002/stem.646 [PubMed: 21563277]
30. Bonnelye E, Chabadel A, Saltel F, & Jurdic P (2008). Dual effect of strontium ranelate: stimulation of osteoblast differentiation and inhibition of osteoclast formation and resorption in vitro. Bone, 42(1), 129–138 [PubMed: 17945546]
31. Gentleman E, Fredholm YC, Jell G, Lotfibakhshaiesh N, O'Donnell MD, Hill RG, & Stevens MM (2010). The effects of strontium-substituted bioactive glasses on osteoblasts and osteoclasts in vitro. Biomaterials, 31(14), 3949–3956 [PubMed: 20170952]
32. Marie PJ (2005). Strontium as therapy for osteoporosis. Current opinion in pharmacology, 5(6), 633–636 [PubMed: 16183330]
33. Reffitt D, Ogston N, Jugdaohsingh R, Cheung HF, Evans BA, Ogston RP, Thompson, … Hampson GN, Orthosilicic acid stimulates collagen type 1 synthesis and osteoblastic differentiation in

human osteoblast-like cells in *vitro*. Bone 2003, 32, 127–135. doi:10.1016/S8756-3282(02)00950-X [PubMed: 12633784]

34. Jugdaohsingh R, Tucker KL, Qiao N, Cupples LA, Kiel DP, Powell JJ, Dietary silicon intake is positively associated with bone mineral density in men and premenopausal women of the Framingham Offspring Cohort. Journal of Bone and Mineral Research, 2004, 19, 297–307. doi: 10.1359/JBMR.0301225. [PubMed: 14969400]
35. Bose S, Robertson SF, & Bandyopadhyay A (2017). Surface Modification of Biomaterials and Biomedical Devices using Additive Manufacturing. Acta Biomaterialia, 11 3.
36. Bobbert FSL, Lietaert K, Eftekhari AA, Pouran B, Ahmadi SM, Weinans H, & Zadpoor AA (2017). Additively manufactured metallic porous biomaterials based on minimal surfaces: A unique combination of topological, mechanical, and mass transport properties. Acta biomaterialia, 53, 572–584 [PubMed: 28213101]
37. Bose S, Ke D, Sahasrabudhe H, & Bandyopadhyay A (2017). Additive Manufacturing of Biomaterials. Progress in Materials Science.
38. Kar A, Raja KS, & Misra M (2006). Electrodeposition of hydroxyapatite onto nanotubular TiO2 for implant applications. Surface and Coatings Technology, 201(6), 3723–3731
39. Kokubo T and Takadama H 2006 How useful is SBF in predicting in vivo bone bioactivity? Biomaterials 27 2907–15 [PubMed: 16448693]
40. Friberg B, Jemt T, & Lekholm U (1991). Early failures in 4,641 consecutively placed Brånemark dental implants: a study from stage 1 surgery to the connection of completed prostheses. International Journal of Oral & Maxillofacial Implants, 6(2
41. ASTM Standard F2792–12a. Standard Terminology for Additive Manufacturing Technologies. ASTM International, West Conshohocken, PA, 2012, DOI: 10.1520/F2792-12A,2012, www.astm.org
42. Thieme M, Wieters KP, Bergner F, Scharnweber D, Worch H, Ndop J, … & Grill WI, Titanium powder sintering for preparation of a porous FGM destined as a skeletal replacement implant. Mater Sci Forum. 1999, 308–374.
43. Torres Y, Trueba P, Pavón JJ, Chicardi E, Kamm P, García-Moreno F, & Rodríguez-Ortiz JA (2016). Design, processing and characterization of titanium with radial graded porosity for bone implants. Materials & Design, 110, 179–187.
44. Balla VK, Bose S A. Bandyopadhyay, Low stiffness porous Ti structures for load bearing implants. Acta biomaterialia, 2007, 3(6), 997–1006. [PubMed: 17532277]
45. Zreiqat H, Valenzuela SM, Nissan BB, Roest R, Knabe C, Radlanski RJ, … & Evans PJ, The effect of surface chemistry modification of titanium alloy on signalling pathways in human osteoblasts. Biomaterials, 2005, 26(36), 7579–7586. [PubMed: 16002135]
46. Ke D, Robertson SF, Dernell WS, Bandyopadhyay A, & Bose S (2017). Effects of MgO and SiO_2 on plasma-sprayed hydroxyapatite coating: An in vivo study in rat distal femoral defects. ACS applied materials & interfaces, 9(31), 25731–25737. [PubMed: 28752993]
47. Su EP, Justin DF, Pratt CR, Sarin VK, Nguyen VS, Oh S, & Jin S (2018). Effects of titanium nanotubes on the osseointegration, cell differentiation, mineralisation and antibacterial properties of orthopaedic implant surfaces. Bone Joint J, 100(1 Supple A), 9–16. [PubMed: 29292334]

Highlights

- Porous Ti implants were processed via LENS™, a commercial 3D printing technique with stiffness, similar to bone.
- A combination of nanoscale surface modification with TiO_2 nanotubes and Sr^{+2}- Si^{+4} doped calcium phosphate coating on these porous implants was studied.
- Porous implants showed better bone tissue integration *in vivo* than the dense ones in a rat distal femur model.
- Calcium phosphate played a significant role to enhance early-stage bone tissue integration.

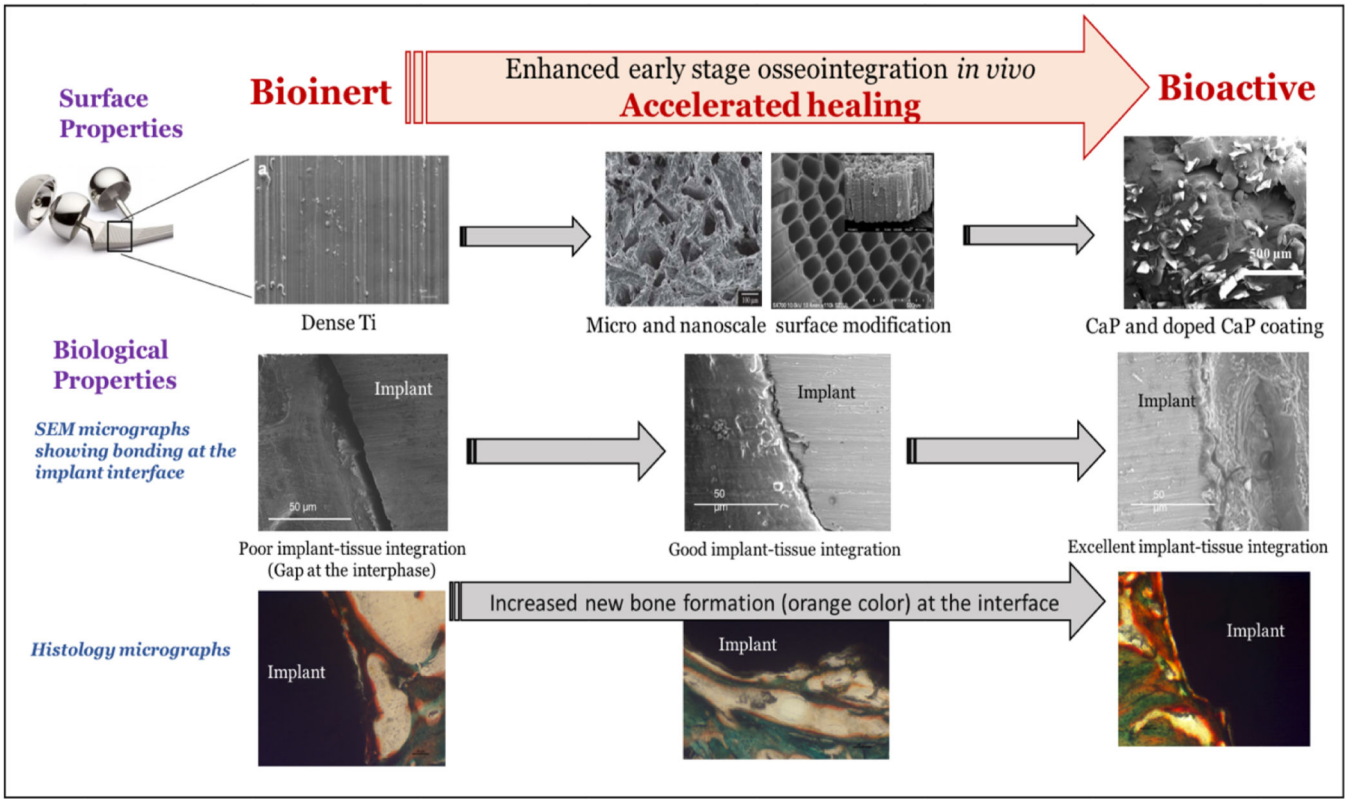

Figure 1.

demonstrates the effects of combination of nanoscale surface modification with doped CaP coating on porous CpTi on *in vivo* osseointegration in a rat distal femur model

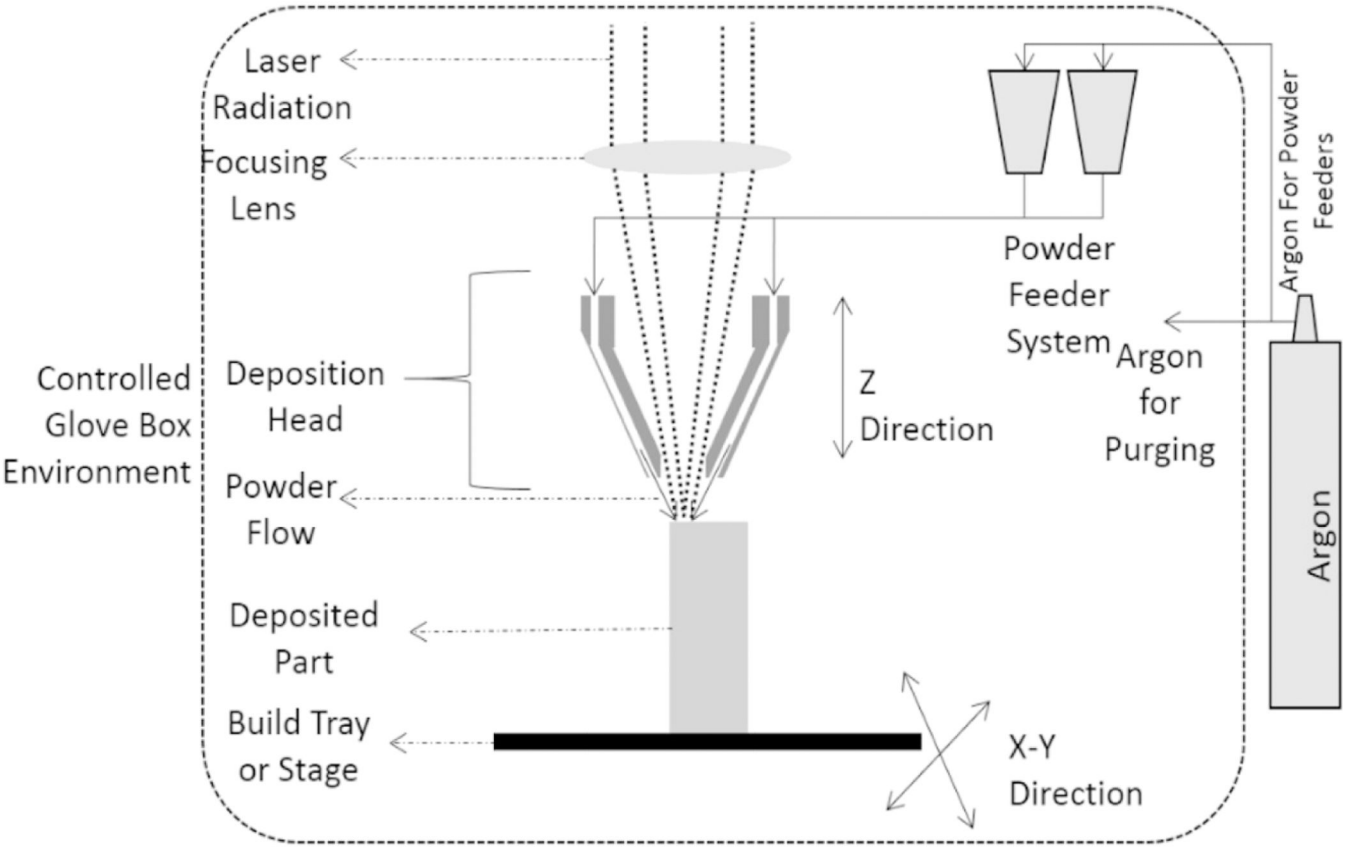

Figure 2:
Schematic representation of the LENS™ process [24].

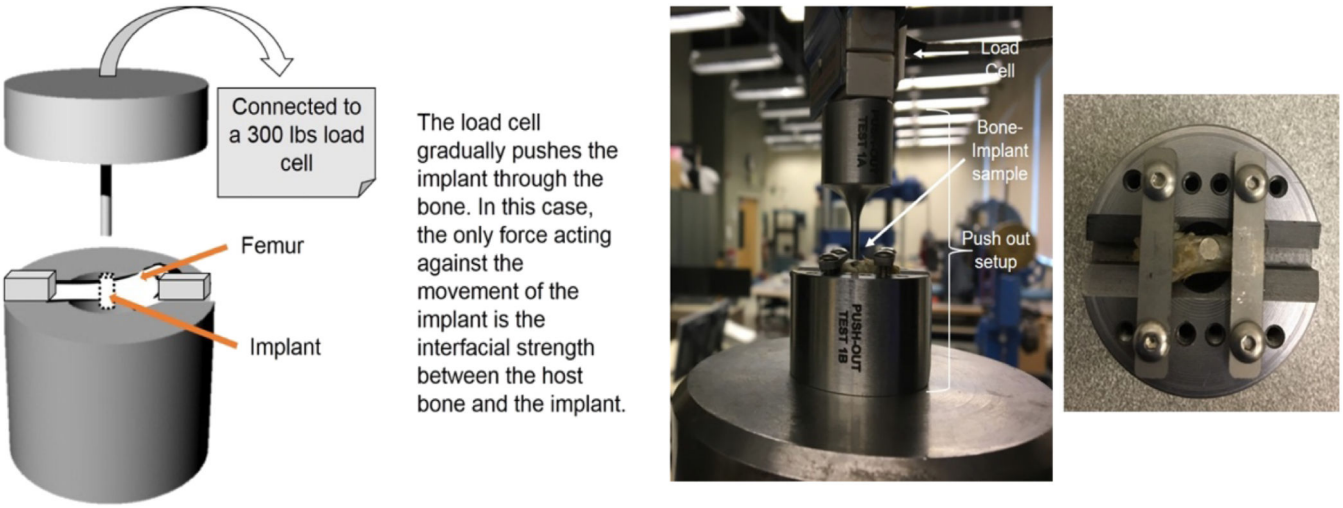

Figure 3:

(a) Schematic of push-out test set-up. (b) Picture of push-out test set-up connected with the Instron. (c) Top view of the push-out test set-up with a sample attached.

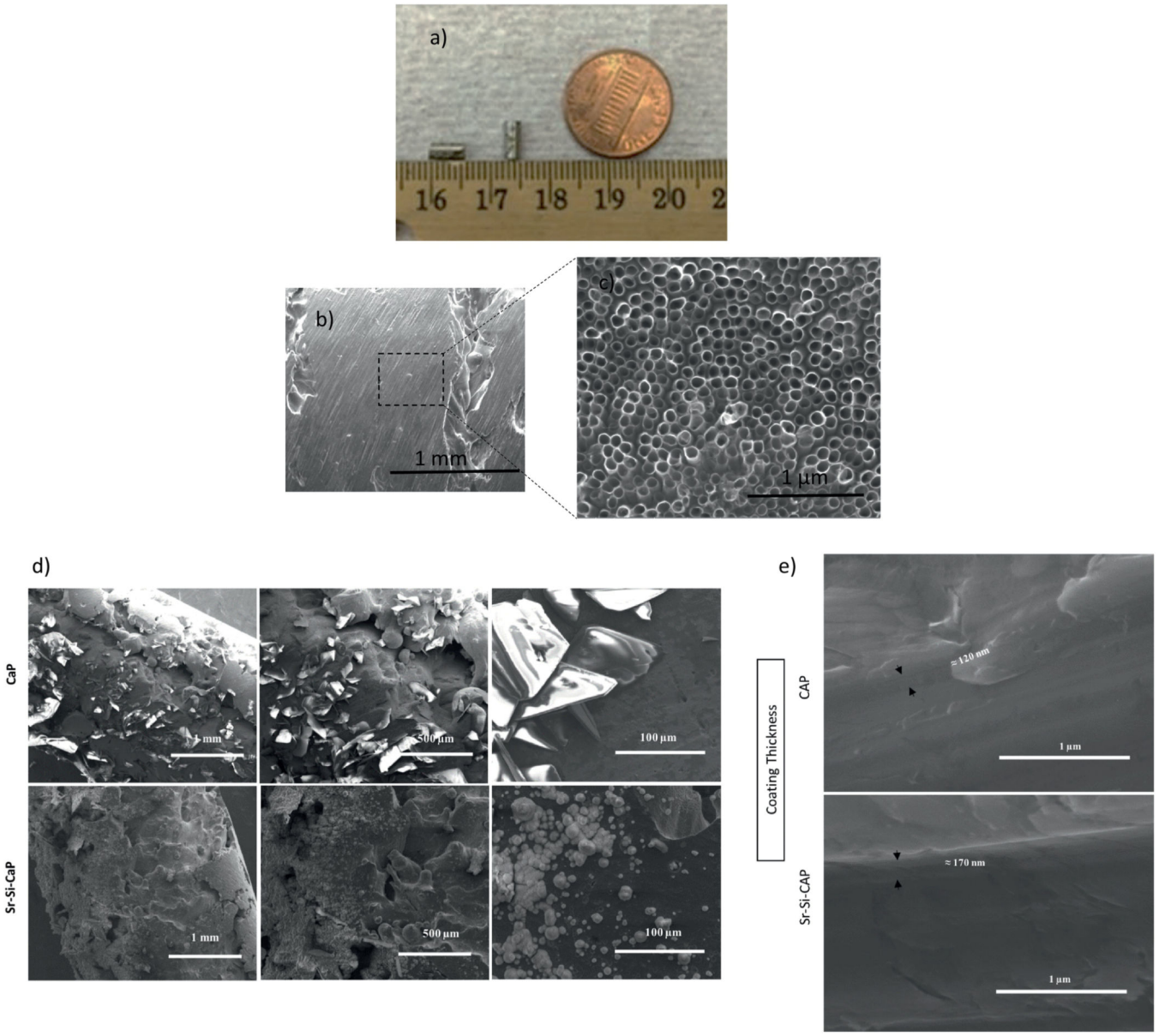

Figure 4.

(a-c):SEM and optical image [24] of the porous surface nature of LENS™ processed porous sample and porous Ti implant with fabrication of nanotubes with diameter 105±30nm and length 375±35nm using anodization method.

(d): CaP and Sr-Si-CaP coating morphology on cylindrical LENS™ Porous Ti-NT samples at different magnifications showing the Sr and Si crystals on the cylinders.

(e): CaP and Sr-Si-CaP coating thickness on cylindrical LENS™ Porous Ti-NT samples showing 120 nm and 170 nm thickness respectively.

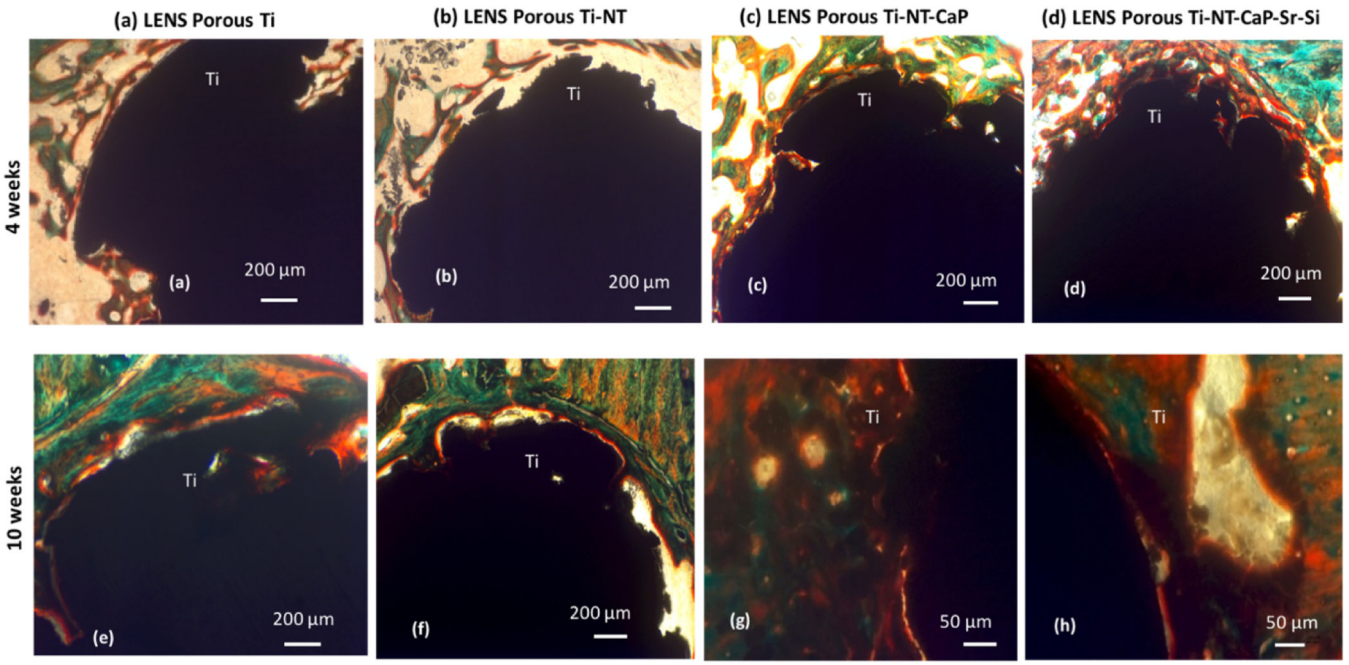

Figure 5:

Signs of osteoid like new bone generation (in reddish orange color) in the histology images after 4 weeks (a, b, c, d) and 10 weeks (e, f, g, h). Modified Masson Goldner's trichrome staining method was used, demonstrating enhanced bone formation in the doped coating at both the time points.

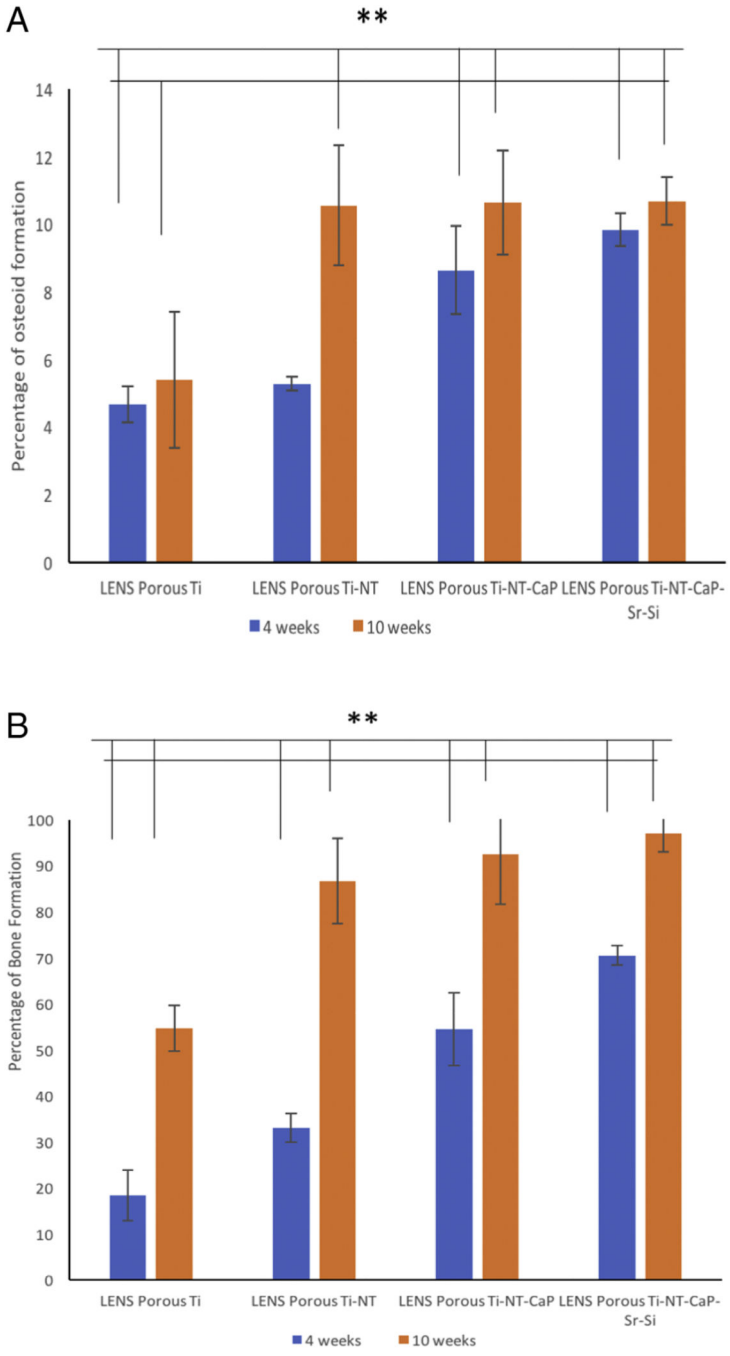

Figure 6.

(a) shows total osteoid formation around the implant (200μms in radius) for the different compositions at two studied time points. (** means P value < 0.001, so statistically significant)

(b) shows total amount of bone formation around the implant (200μms in radius) for the different compositions at two studied time points (** means P value < 0.001, so statistically extremely significant).

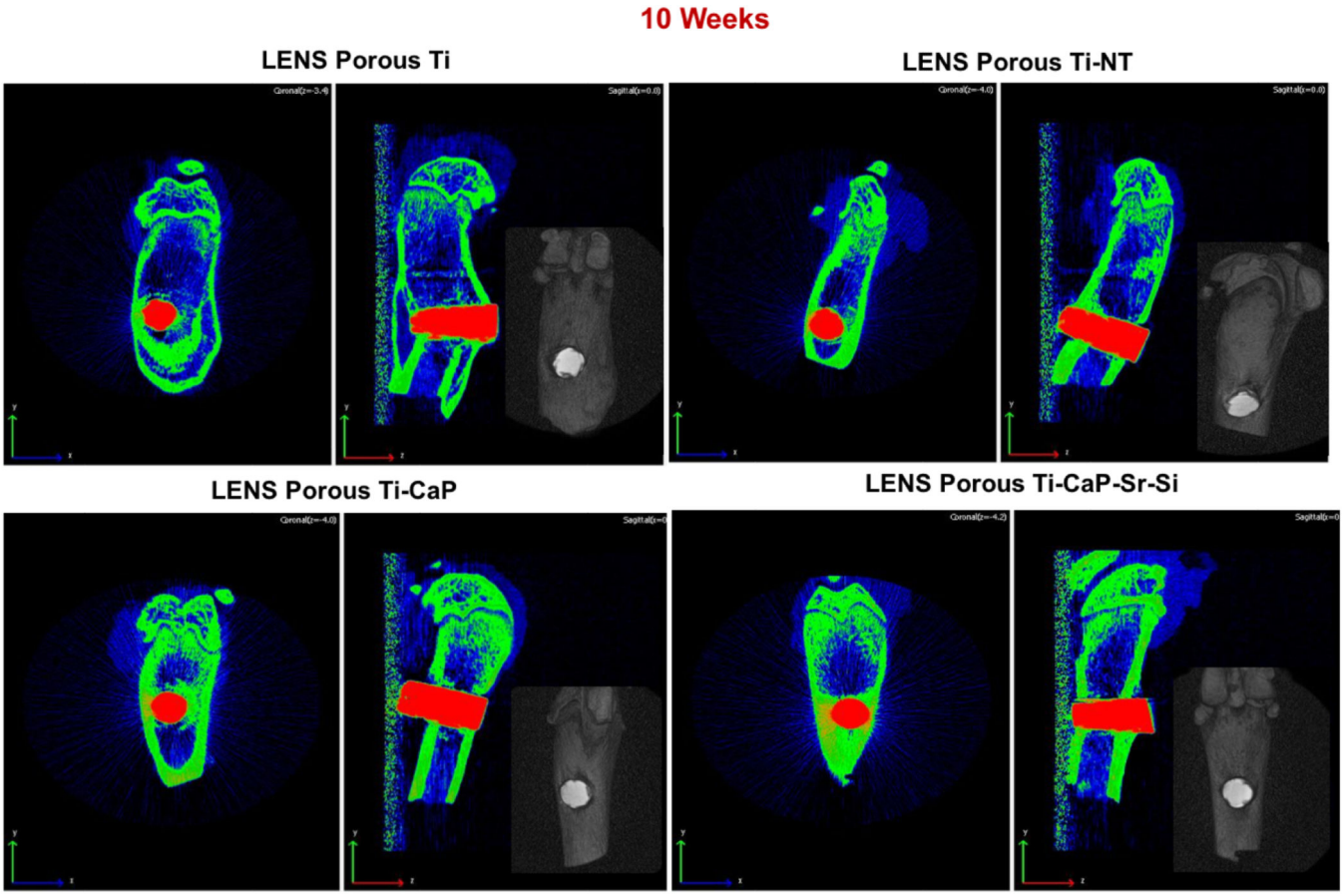

Figure 7:
CT scan images of implants after 10 weeks showing tissue ingrowth into the implants with no notable defects or gaps along the interface in the doped coating. (n=2)

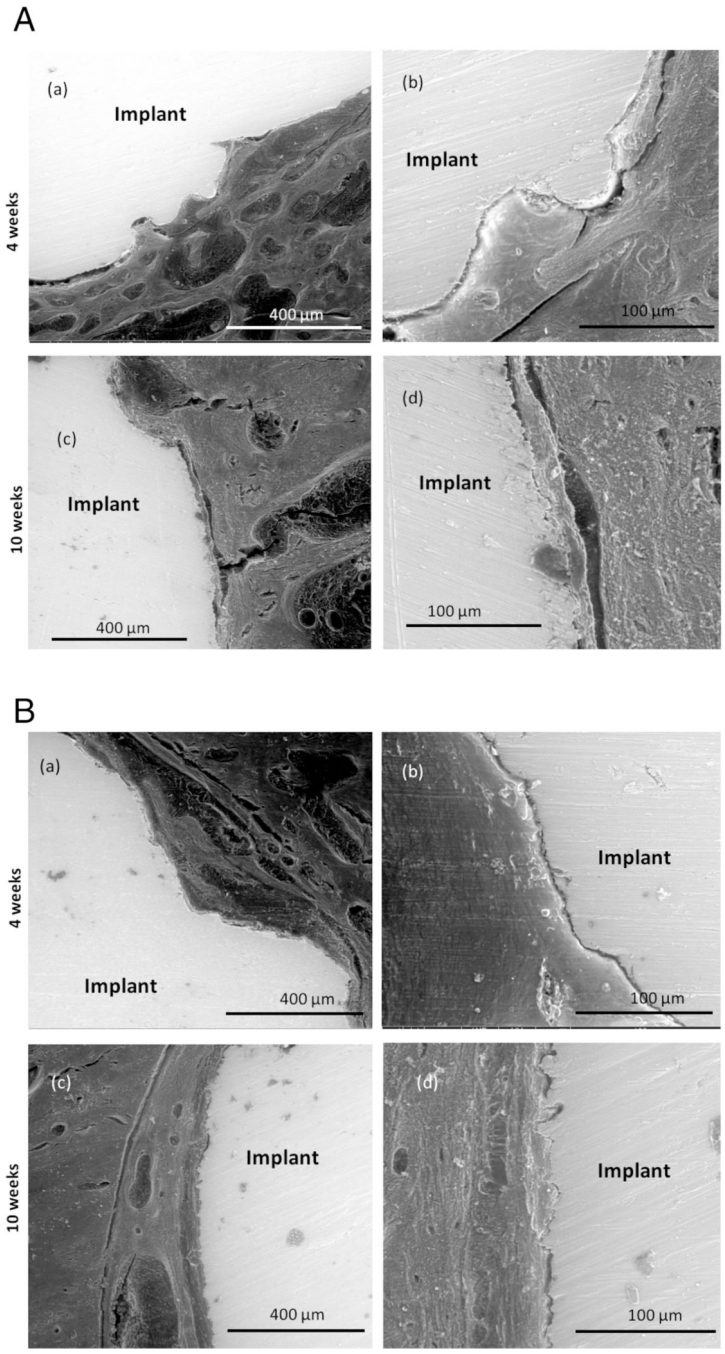

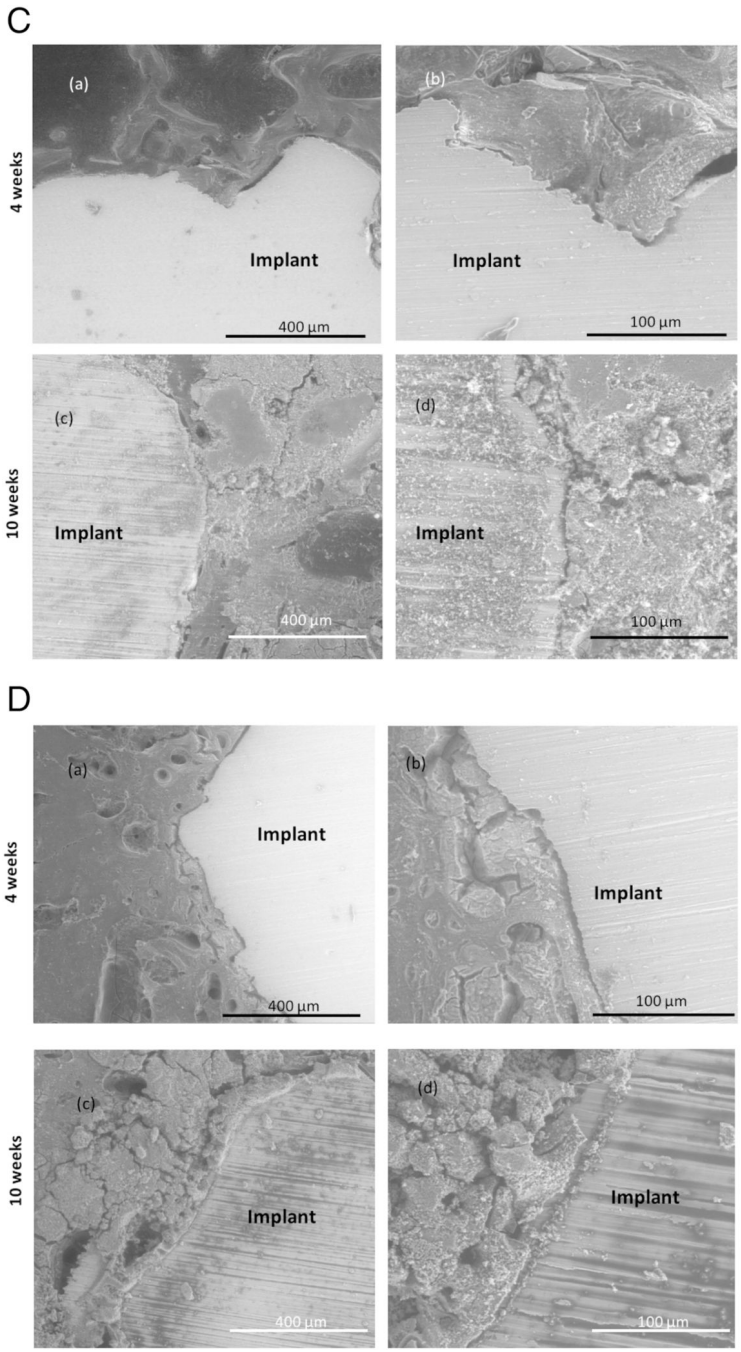

Figure 8.

(A):SEM images of stained porous Ti samples after 4 (a, b) and 10 (c, d) weeks showing the interfacial bonding between the implant and the tissue.

(B): SEM images of stained porous Ti-NT samples after 4 (a, b) and 10 (c, d) weeks showing the interfacial bonding between the implant and the tissue.

(C): SEM images of stained porous Ti-NT-CaP samples after 4 (a, b) and 10 (c, d) weeks showing the interfacial bonding between the implant and the tissue.

(D): SEM images of stained porous Ti-NT-CaP-Sr-Si samples after 4 (a, b) and 10 (c, d) weeks showing the interfacial bonding between the implant and the tissue.